Quantum interferometry for different energy landscapes in a tuneable Josephson junction circuit

Pernel Nguenang,[1] Michael Nana Jipdi,[1,2] Patrick Louodop,[1,3] Martin Tchoffo,[1,4] Lukong Cornelius Fai,[1] and Hilda A. Cerdeira[3]

[1)] *Research Unit Condensed Matter, Electronics and Signal Processing, Université de Dschang, P.O. Box 67 Dschang, Cameroon*

[2)] *Department of physics, Higher Teacher Training College, University of Bamenda, P.O. 39 Bambili, Cameroon*

[3)] *São Paulo State University (UNESP), Instituto de Física Teórica, Rua Dr. Bento Teobaldo Ferraz 271, Bloco II, Barra Funda, 01140-070 São Paulo, Brazil*

[4)] *Centre d'Études et de Recherches en Agronomie et en Biodiversité, Faculté d'Agronomie et des Sciences Agricoles, University of Dschang, P.O. 222 Dschang Cameroon*

(Dated: 1 October 2020)

This paper presents a simple Josephson-junction circuit with two parameters (inductance and capacitance) which can be tuned to represent different energy landscapes with different physical properties. By tuning this quantum circuit through external accesible elements we can move from two to three and more energy levels depending on the parameter setting. The inductance, the capacitance as well as the external voltage (driving terms) condition the number of relevant energy levels as well as the model to be used. We show that the quantized circuit represents a multi-level system with tunneling induced by the Landau-Zener and Landau-Zener-Stückelberg transition. The special cases of single crossing and multi-crossing models are thoroughly studied and the transition probability is obtained in each case.

It is proven that, the crossing time as well as the relaxation time affect drastically the transition probability; the system mimics a single passage for short relaxation and a multiple passage problem for large relaxation. The nonlinearity of energy levels modifies the transition probability and the derived adiabatic parameters help to redefine the Landau-Zener probability. The observed constructive and destructive interference are parametrically conditioned by the initial condition set by the inductive branch. Moreover, the total population transfer as well as the complete blockage of the system are obtained in a permissible range of parameters only by changing the values of the inductance. Therefore, the system model a controllable level-crossing where the additional branches (inductive and capacitive) helps in designing the number of levels, the type of interferometry as well as the control of levels' occupation.

I. INTRODUCTION

The Josephson effect, predicted in 1962 by B.D. Josephson[1], is a phenomenon that occurs when two superconductors are separated by a very thin layer of non-superconductive material. A superconducting current passes through the barrier and the electrical properties of this system are very precisely defined[2]. This current depends on the phase difference between the superconductors and it has been observed experimentally by P.L. Anderson and J.W Rowel[3] and called Josephson's current[4]. Furthermore, if we apply a constant voltage to this junction, an alternating current is created and it was experimentally demonstrated by S. Saphiro in 1963[5].

It has been demonstrated that the well-known Josephson effect is a result of the quantum tunnelling[2,6–9]. In fact, Josephson's effect is a macroscopic observation of the tunnelling effect of condensed electron pairs between the Fermi surfaces of two metals through a thin barrier. From another perspective, quantum tunnelling is a well-known phenomenon where a particle crosses a potential barrier higher than its own energy[10]. There exist applications in many fields of physics, chemistry and biology[11,12]. The quantum tunnelling phenomenon is the key point of quantum computing and has also been used in characterizing dynamical behaviour across Josephson junctions[13–16]. The phenomenon gained a lot of interest in the two last decades[17] in the investigation of properties of superconducting devices[18–27]. One of the prominent applications of the Josephson junction is found in quantum computing where the resulting physical system when modelled as a qubit-qubit is helpful in implementing logic gates, as well as quantum transistors[28,29]. This is achieved by modelling Josephson circuits as two or multilevel systems[30,31]; some examples include traditional two-level systems[32], flux qubits[33], charge qubits[34], Cooper-pair box[35,36] and three level systems[37]. In these set-ups, due to external sources (current or voltage), the tunnelling occurring is of the Landau Zener type.

In the early 1930's, Landau and Zener developed a possible transition between two similar levels because of a control-value scanned at the point of minimum energy splitting[35,38,39]. The Landau-Zener effect is at the basis of several quantum mechanical processes, and it was recently discovered in periodic structures, with applications in driven superlattices[40],current driven Josephson junction[41] and bosonic systems[42–44]. The Landau-Zener tunneling occurs at the crossing of two energy levels which move away due to a weak interaction[35], and it has largely been investigated for particular configurations

such as external field influence, periodic modulation[45,46], non-linear models[42,43,47,48], multi-level models[37,49] and multi-crossing model in its multiple configurations (real or fictitious crossing)[50–52] and it still gains a lot of attention due to its prominent uses.

From another perspective, level crossing systems often show avoided energy level (anti-crossing) which can be handled using an external control-value[53]. When the energy level in a given region has a double crossing, the accumulation phase between transitions generates either a destructive or constructive interference in the time domain, called Stückelberg oscillations[54,55]. When such a level crossing system is subjected to a periodic driving force, the physical observables of the system show a periodic dependence that mimics the Landau-Zener-Stückelberg interferometry[51]. Landau-Zener-Stückelberg interferometry is therefore the realization of an interferometer with an energy spectrum having at least two bands or branches, separated by a gap[56]. The Landau-Zener Stückelberg interferometry has been demonstrated for superconducting qubits[53,57], a Cooper-pair box[35,36], nitrogen deficiency centers[58], and quantum dots[59,60]. The Landau-Zener-Stückelberg interferometry is of major importance in quantum computation since its helps in the design of controllable modulus and also confer a better read out for quantum logic gates[50,61].

In the present work, we shall show that a simple electrical circuit with a single Josephson junction assisted by controllable parameters (inductance and capacitance) and under a periodic force will present the abovementioned phenomena. The main objective of this work is to show how the resulting modified Josephson junction can model either a controllable two or multi-level system where quantum tunnelling is induced by the Landau-Zener scenario. The resulting quantum interferometer is defined and the conditions for constructive and destructive interferences is investigated.

The rest of this paper is organized as follows: Sec.II presents the electronic circuit and describe the elements. In section III, we focus on the construction of the Hamiltonian of the system based on the range of values of controllable parameters. Sec.IV is devoted to quantum tunnelling and the evaluation of level occupation in different set-ups (two-level and multi-level); interference is also investigated. Sec.V presents the summary of the work.

II. CIRCUIT AND MODEL: DESCRIPTION OF CIRCUIT ELEMENTS

The electrical circuit that we are analyzing is given by the following graph (See Fig.1) as presented in[62].

Summarizing, a single-component Josephson junction (JJ) (blue part of the circuit[63–68]) connected in parallel to a coil of inductance L, which is part of the C_1-L-C_2 tank circuit series with a periodic force, while the Josephson junction, the nonlinear element, plays the feedback loop[62]. Applying Kirchhoff's law on the circuit on Fig.1,

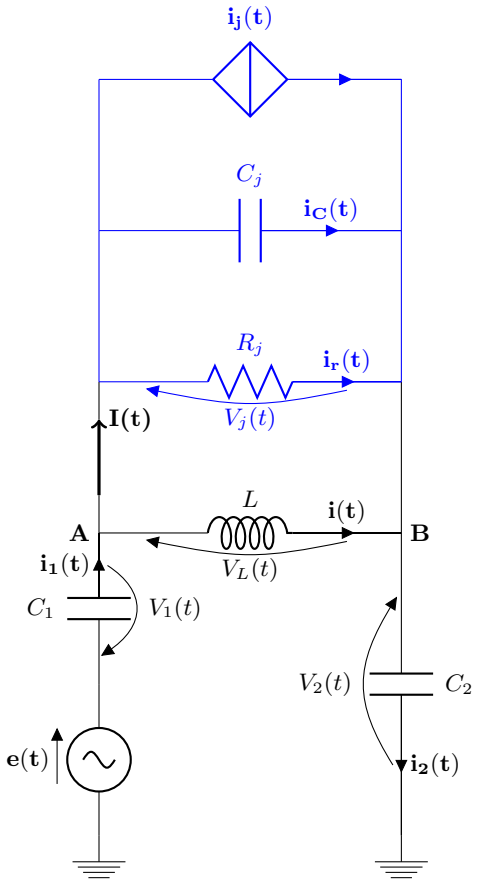

FIG. 1. Josephson junction based circuit[62]

we obtain the following expressions:

$$\frac{\Phi_0}{2\pi}\dot{\phi}(t) = V_j(t) \tag{1a}$$

$$\dot{V}_j(t) = \frac{2C}{C+2C_j}\left(\frac{\dot{e}(t)}{2} - \frac{i_s}{C}sin(\phi) - \frac{V_j(t)}{R_jC}\right) - \frac{2C}{C+2C_j}\left(\frac{\Phi_0}{2\pi}\frac{1}{LC}\phi(t) - p\right), \tag{1b}$$

where ϕ and V_j are respectively the phase and the voltage of the Josephson junction and the constant p is expressed as: $p = \frac{1}{LC}\phi(0) - \frac{1}{C}i(0)$. The capacitors C_1 and C_2 are assumed identical and equal to C. $\frac{\Phi_0}{2\pi}$ is the quantum flux.

To facilitate discussions, we define new variables: $x_1 = \phi(t)$, $P_1(t) = \frac{\Phi_0}{2\pi}C_jV_j(t)$, e_0 is the amplitude of $\frac{\dot{e}(t)}{2}$, $\tau = \Omega t$, $\beta = \frac{2C}{C+2C_j}\frac{\Phi_0}{2\pi}$, $a_1 = \frac{i_s}{C}$, $\mu = \left(\frac{\Phi_0}{2\pi}\right)^2 C_j$, $a_3 = \frac{\Phi_0}{2\pi}\frac{1}{LC}$, such that the circuit represented in Fig.1 is well represented by the dimensionless generalized coordinates

:

$$\begin{aligned}\mu\dot{x}_1(\tau) &= P_1(\tau)\\ \dot{P}_1(\tau) &= \beta\left(e_0 sin(\Omega\tau) - a_1 sin(x_1(\tau)) - a_3 x_1(\tau) - p\right).\end{aligned} \tag{2}$$

Here, C_j is the capacitance of the capacitor parallel to the Josephson junction component. It is the first controllable parameter that conditions the value of the charging energy $\frac{\hbar^2}{2\mu}$ as well as the energy stored in the junction βa_1 through parameters β and μ.

L is the inductance of the coil parallel to the Josephson junction component; it is the second controllable parameter that conditions the shape of the potential energy and therefore, the level configuration as well as the number of levels through the a_3 parameter.

The parameter p carries the initial conditions in the inductive branch. It is helpful in the design of constructive and destructive interferences. $e_0 sin(\tau)$ is the periodic force (external source) that induces the time dependence of energy levels and conditions the avoided crossing on the energy-time graph.

III. HAMILTONIAN MODELLING

To study the microscopic phenomenon that conditions the behaviour of the circuit, we focus on hermitian contributions and ignore dissipative terms (that means R_j is very large). Representing Eq.(2) as the Hamilton's equation with generalized coordinates (x_1, P_1), the Hamiltonian of the system is given by:

$$\begin{aligned}H(x_1, P_1) =& \frac{1}{2\mu}{P_1}^2 + \beta\left(p - f\left(t\right)\right)x_1 + \beta a_1 \cos\left(x_1\right)\\ &+ \beta a_3 \frac{x_1^2}{2},\end{aligned} \tag{3}$$

and the Lagrangian

$$L(x_1, P_1) = \frac{1}{2\mu}{P_1}^2 - \beta\left(p - f\left(t\right)\right)x_1 - \beta a_1 \cos\left(x_1\right) - \beta a_3 \frac{x_1^2}{2}. \tag{4}$$

Here, x_1 plays the role of coordinates while P_1 is the particle momentun and from canonical quantization (first quantization) $[x_1, P_1] = i\hbar$ and $P_1 = -i\hbar\frac{\partial}{\partial x_1}$. From the Lagrangian of the system, we deduce in terms of x_1 the dimensionless confining static potential:

$$\begin{aligned}U(x_1) =& \frac{2\mu}{\hbar^2}\left(\beta p - \beta f\left(t\right)\right)x_1 + \frac{2\mu}{\hbar^2}\beta a_1 \cos\left(x_1\right)\\ &+ \frac{2\mu}{\hbar^2}\beta a_3 \frac{x_1^2}{2}.\end{aligned} \tag{5}$$

The shape of the confining potential is conditioned by the tunable parameters (inductance L, capacitance C and C_j) through parameters β, a_1, μ and a_3 ; two particular cases are observed:

Firstly, the effective charging energy of the system is greater than the effective energy stored in the Josephson junction. ($\frac{2\mu}{\hbar^2}\beta a_1 \ll 1$ and $a_1 \gg a_3$). Here, the last two terms of the Hamiltonian act as a perturbation to the self consistent part.

In the second case, the effective charging energy of the system is smaller than the effective energy stored in the Josephson junction. ($\frac{2\mu}{\hbar^2}\beta a_1 \gg 1$ and $a_1 \gg a_3$). Here, the last two terms of the Hamiltonian can no more be treated as a perturbation but as a part of the self consistent Hamiltonian. It is instructive to mention that the condition $a_1 > a_3$ is very crucial for the appearance of multiple potential wells; if $a_1 \leq a_3$ and no matter the value of $\frac{2\mu}{\hbar^2}\beta a_1$, we obtain a modified single harmonic potential and therefore no tunnelling barrier. These situations are depicted in Fig.2 and Fig.3.

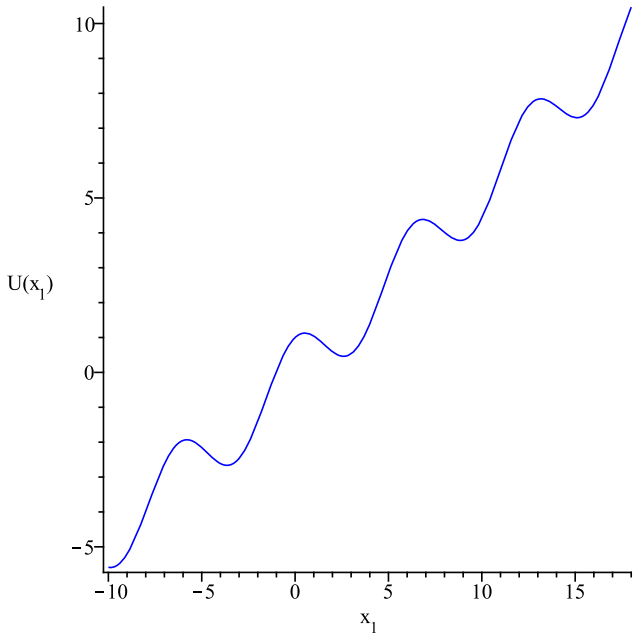

FIG. 2. Schematic representation of the potential with respect to x_1. $\frac{2\mu}{\hbar^2}\beta = 0.25$; $a_1 = 2$; $p = 1$; $a_3 = 0.01$.

In Fig.2, we present the case where the effective charging energy of the system is greater than the effective energy stored in the Josephson junction ($\frac{2\mu}{\hbar^2}\beta a_1 \ll 1$). The diagram presents several minima with different energies; each minimum represents a possible phase state and the system can be modelled as a multi-level one.

In Fig.3 ($\frac{2\mu}{\hbar^2}\beta a_1 \gg 1$), we find only two relevant energy minima; the remaining curvature do not present any dept and cannot be considered as a confining well. The system can be modeled as a two-level system with a different ground state energy[69].

It is instructive to mention that, the number of levels in the system is conditioned by the inductance value. From a deeper investigation, if $\frac{a_3}{a_1} > 1$, the system mimics a simple harmonic potential, the system is devoid of potential barrier. If $0.1284374 < \frac{a_3}{a_1} < 1$ ($a_3 < a_1$), the

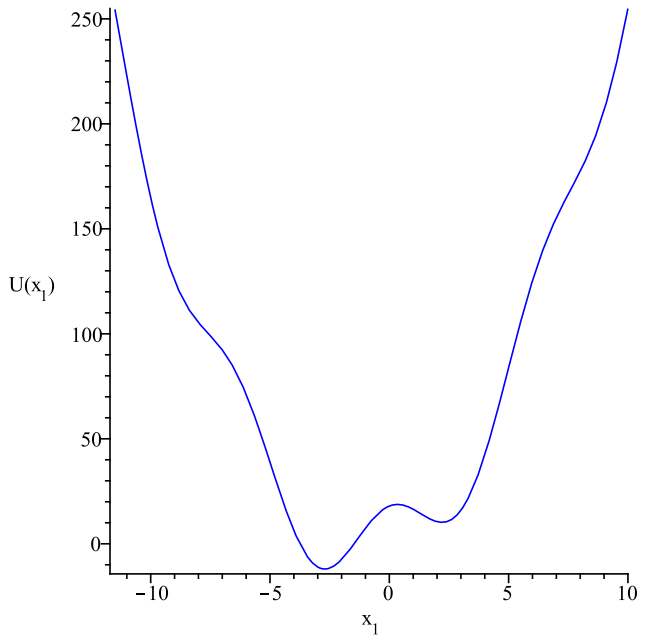

FIG. 3. Schematic representation of the potential with respect to x_1. $\frac{2\mu}{\hbar^2}\beta = 9$; $a_1 = 2$; $p = 1$; $a_3 = 0.5$.

system presents two energy minima; the supplementary curvature do not present any deepness and the confining potential is a double well; this is helpful in designing a two-level system. If $0.0709134 < \frac{a_3}{a_1} < 0.1284374$ $(a_3 < a_1)$, the system has four energy minima and can therefore be modelled as a four-level system; $0.0490296 < \frac{a_3}{a_1} < 0.0709134$, we have six minima so a six-level system; $0.0374745 < \frac{a_3}{a_1} < 0.0490296$, the system presents eight levels; we can easily realise that the smaller the factor $\frac{a_3}{a_1}$, the larger the number of energy minima and consequently the number of levels.If that factor is exceedingly small, we have an infinite number of levels describing the situation in Fig.2.

These particular behaviours are obtained from a single Josephson junction circuit only by playing on tuneable parameters that are the inductance L and the capacitance (C and C_j). Therefore, when $\frac{2\mu}{\hbar^2}\beta a_1 < 1$ we resume the condition as $\frac{4C_j}{C+2C_j} < \frac{\hbar^2}{i_s}\left(\frac{2\pi}{\Phi_0}\right)^3$; for $a_3 < a_1$, we design as $\frac{\phi_0}{2\pi} < Li_S$; here, the effective charging energy of the system is larger than the effective energy stored in the junction. This condition is achieved by reducing the frequency Ω of generator for the process to be adiabatic and reducing the capacitance C_j and enhancing the inductance L. When the capacitance C_j is enhanced, $\frac{4C_j}{C+2C_j}$ is large; the effective energy stored in the junction becomes large and can no more be considered as a perturbation; the number of levels of system is reduced and a two-state system is achieved for $0.1284374 < \frac{a_3}{a_1} < 1$ with the confining potential represented by a double well (see Fig.3).

A. Large effective charging energy

When the effective charging energy of the system is greater than the effective energy stored in the Josephson junction then $\frac{2\mu}{\hbar^2}\beta a_1 \ll 1$ and $a_1 \gg a_3$.

In this situation, the shape of the potential is given in Fig.2 and the Hamiltonian is given by

$$H = \frac{1}{2\mu}{P_1}^2 + \beta a_1 \cos(x_1) + \beta a_3 \frac{x_1^2}{2} + \beta\left(p - f(t)\right)x_1. \quad (6)$$

Since $\frac{2\mu}{\hbar^2}\beta a_1 \ll 1$ and $a_1 \gg a_3$ then, the two last terms of the Hamiltonian are considered as a perturbation and the unperturbed part can be labeled as H_0 therefore,

$$H = H_0 + V_1,$$

where

$$H_0 = \frac{1}{2\mu}{P_1}^2 + \beta a_1 \cos(x_1),$$

$$V_1 = \beta a_3 \frac{x_1^2}{2} + \beta\left(p - f(t)\right)x_1.$$

To quantize this Hamiltonian, we use the displacement operator and write down the wave function as follows:

$$\psi(x_1, t) = \varphi(x_1, t)\, exp\left[-\frac{i}{\hbar}\int \beta\left(p - f(t)\right)x_1 dt\right]. \quad (7)$$

The effective Hamiltonian of the perturbed system is reduced to:

$$H = \frac{1}{2\mu}\left(P_1 - F(t)\right)^2 + \beta a_1 \cos(x_1) + \beta a_3 \frac{x_1^2}{2}, \quad (8)$$

with

$$F(t) = \int \beta\left(p - e_0 \sin(\Omega t)\right) dt. \quad (9)$$

The Schrödinger equation of the unperturbed part is

$$\frac{\partial^2 \psi_m}{\partial x^2} + \left(\frac{2\mu E_m}{\hbar^2} - \frac{2\mu\beta a_1 \cos(x)}{\hbar^2}\right)\psi_m = 0. \quad (10)$$

Because of intrinsic parity of the potential, the solution is characterized by an even function. The solution of this equation is the well known periodic Mathieu function[70] given by

$$\psi_m = ACe_{i_m}\left(\frac{2\mu\beta a_1}{\hbar^2}, x\right), \quad (11)$$

or in terms of series

$$Ce_{i_m} = \sum_{n=0}^{\infty} A_n^{(m)} \left(\frac{2\mu\beta a_1}{\hbar^2}\right) \cos(mx).$$

The unperturbed wave function is then a linear combination of cosine functions; since $\frac{2\mu\beta a_1}{\hbar^2} \ll 1$, the energy of the unperturbed part is[71,72].

$$\frac{2\mu E_m}{\hbar^2} \sim m^2 + \frac{(2\mu\beta a_1)^2}{2\hbar^4(m^2-1)},$$

or

$$E_m \sim \frac{\hbar^2}{2\mu} m^2 + \frac{\mu(\beta a_1)^2}{\hbar^2(m^2-1)}.$$

The second part of the energy is just the perturbation (very small) and the system mimics a high energy quantum rotor. From the wave function in Eq.(11), we can build the solution of the system inducing the perturbation (V_1) as a linear combination of cosine functions but with variable coefficients. Therefore,

$$\psi_m = \sum_m \frac{A_m(t)}{\sqrt{\pi}} \cos mx.$$

This wave function satisfies the time dependent Schrödinger equation; which when multiplied by the factor $\frac{1}{\sqrt{\pi}} \cos nk$ and the integral over $0 \prec x \prec 2\pi$ one has

$$i\hbar\frac{\partial}{\partial t}\dot{A}_n(t) = \frac{\beta a_1}{2}\left(A_{n-1} + A_{n+1}\right) + \sum_m \beta a_3 \frac{1}{(n-m)^2} A_{n-m} + \\ + \sum_n \frac{(\hbar m - F(t))^2}{2\mu} A_n.$$

We observe that the additional coupling factor($\beta a_3 \frac{1}{(n-m)^2}$) decays quickly when the difference between quantum numbers $(m-n)$ is large; since a_3 is chosen to be very small, only the nearest neighbour are relevant and enables us to write the effective Hamiltonian

$$\mathcal{H} = \sum_m \epsilon_m A_m^\dagger A_m + \Delta\left(A_m^\dagger A_{m-1} + A_m^\dagger A_{m+1}\right),$$

or in terms of states:

$$\mathcal{H} = \sum_m \epsilon_m |m\rangle\langle m| + \Delta\left(|m\rangle\langle m-1| + |m\rangle\langle m+1|\right) \tag{12}$$

with

$$\epsilon_m = \frac{4\pi^2}{3}\beta a_3 + \frac{1}{2\mu}(\hbar m - F(t))^2,$$

$$\Delta = \frac{\beta a_1}{2} + \frac{\beta a_3}{2}.$$

Focusing only on states $m = 0$, $m = 1$ and $m = -1$, the electronic circuit mimics a three-level system:

$$\mathcal{H} = \begin{pmatrix} \epsilon_{-1} & \Delta & 0 \\ \Delta & \epsilon_0 & \Delta \\ 0 & \Delta & \epsilon_1 \end{pmatrix}. \tag{13}$$

ϵ_{-1} , ϵ_0 and ϵ_1 are the energies of the three relevant states; Δ stands for the energy gap.

If all the states are considered as relevant, the system mimics a multi-level system with an infinite number of levels represented by the Hamiltonian as follow:

$$\mathcal{H} = \sum_m \epsilon_m |m\rangle\langle m| + \Delta\left(|m\rangle\langle m-1| + |m\rangle\langle m+1|\right)$$

B. Low effective charging energy

In the case where the effective charging energy of the system is less than the effective energy stored in the Josephson junction, the factor $\frac{2\mu}{\hbar^2}\beta a_3$ is large and the shape of the confining potential changes drastically (double well potential Fig.3). This is achieved by reducing the value of the capacitance C and the inductance L. The Hamiltonian of the system is given as in Eq.8

To analyse the form of the wave function, we take

$$H_0 = \frac{1}{2\mu}{P_1}^2 + \beta a_1 \cos(x_1),$$

the corresponding eigenfunctions of this part are periodic Mathieu wave function:

$$Ce_{im} = \sum_m^{\infty} A_n^m(q) \cos(mx),$$

but in this configuration $\frac{2\mu}{\hbar^2}\beta a_1 \gg 1$ therefore, the energy spectrum of the system[71,72]:

$$\frac{2\mu\epsilon_m}{\hbar^2} \simeq -\left(\frac{4\mu\beta a_1}{\hbar^2}\right) + (2n+1)\left(\frac{2\mu\beta a_1}{\hbar^2}\right)^{\frac{1}{2}},$$

so

$$\epsilon_m \simeq 2\beta a_1 + \hbar\Omega_\beta\left(n + \frac{1}{2}\right), \Omega_\beta = \left(\frac{\beta a_1}{8\mu}\right)^{\frac{1}{2}}.$$

The latter corresponds approximatively to the solution of a particle in a harmonic potential. The eigenfunction of the whole system can then be described by the Hermite polynomial

$$\phi_n(x) \sim \left(\frac{\beta}{2^n n!\sqrt{\pi}}\right)^{\frac{1}{2}} H_n(\beta n) \exp\left(\frac{-\beta^2 x^2}{2}\right).$$

Since the junction operates at very low temperature, only the ground state ($n = 0$) is relevant. Observing Fig.3, we have two states corresponding to the ground state of each potential well and described by the left and right wave functions

$$\phi_R(y) = \left(\frac{k}{\sqrt{\pi}}\right)^{\frac{1}{2}} exp\left(-\frac{k^2}{2}y^2\right),$$

$$\phi_L(z) = \left(\frac{k}{\sqrt{\pi}}\right)^{\frac{1}{2}} exp\left(-\frac{k^2}{2}z^2\right),$$

with $k = \left(\frac{\mu\Omega_\alpha}{\hbar}\right)^{\frac{1}{2}}$ and $\Omega_\alpha^2 = \frac{\beta}{\mu}\left(a_3 - \sqrt{a_1^2 - a_3^2\alpha^2}\right)$. $y = x_1 + \alpha$ and $z = x_1 - \alpha$ are two new variables that help to center the wave function with the bottoms of the double well. The bottoms are located at $x_1 = \pm\alpha$.

The global wave function of our system is now written as a superposition of all possible states:

$$\psi = C_R|\psi_R(y)\rangle + C_L|\psi_L(z)\rangle. \tag{14}$$

The wave function (14) can now be used and the time dependent Schrödinger equation for the perturbed system gives:

$$i\hbar\frac{dC_L}{dt} = \epsilon_L(t)\,C_L + \Delta_0 C_R,$$
$$i\hbar\frac{dC_R}{dt} = \epsilon_R(t)\,C_R + \Delta_0 C_L,$$

with

$$\epsilon_L = \epsilon_0 - \alpha\beta(p - f(t)),$$
$$\epsilon_R = \epsilon_0 + \alpha\beta(p - f(t)),$$
$$\Delta_0 = exp(-k\alpha^2)\left(\frac{\beta a_3}{2k} + \beta a_1 exp(-\frac{1}{4k}) + \frac{\hbar^2}{4\mu}\left(1 - 2k\alpha^2\right)\right),$$

where α is the solution of the nonlinear equation $a_1\sin(\alpha) - a_3\alpha = 0$; the term 2α is the width of the barrier between the two wells. ϵ_0 is a constant energy shift with no relevance as far as probability is concerned.

The Hamiltonian of the system is then written as follows:

$$\mathcal{H}_{eff} = \epsilon_L(t)\,{C_L}^\dagger C_L + \epsilon_R(t)\,{C_R}^\dagger C_R + \Delta_0(\alpha)\,{C_R}^\dagger C_L + \Delta_0(\alpha)\,{C_L}^\dagger C_R.$$

This is the Hamiltonian of a two-level system that can also be rewritten in terms of Pauli matrix

$$\mathcal{H}_{eff} = \alpha\beta(p - f(t))\sigma_z + \Delta_0\sigma_x + \epsilon_0. \tag{15}$$

The system mimics the flux qubit or Cooper-pair box with two relevant states[33,35,36].

IV. QUANTUM TUNNELING: SURVIVAL AND TRANSITION PROBABILITIES

In order to investigate the quantum tunneling occurring in the system, we focus on the two models mentioned above. For each of these configurations, the system is isolated and therefore the study related to decoherence are omitted; the transition probabilities will be investigated for each cases.

A. Two-level system

The two-level system is obtained when $\frac{2\mu}{\hbar^2}\beta a_1 \gg 1$ and $a_1 \gg a_3$. To achieve this, we reduce the capacitance C_j as well as the inductance L so that $\frac{4C_j}{C+2C_j}\frac{i_s}{\hbar^2}\left(\frac{\Phi_0}{2\pi}\right)^2 \gg 1$. The Hamiltonian of the system is given by

$$\mathcal{H}_{eff} = (\epsilon_0 - \alpha\beta(f(t) - p))\,{C_L}^\dagger C_L + \Delta_0 {C_L}^\dagger C_R + \Delta_0 {C_R}^\dagger C_L + (\epsilon_0 + \alpha\beta(f(t) - p))\,{C_R}^\dagger C_R.$$

To solve the problem, we make use of the dynamic matrix approach[73]. We introduce the field vector of the system as $\psi = \begin{pmatrix} C_L\,|L\rangle \\ C_R\,|R\rangle \end{pmatrix}$ with $\psi_0 = \begin{pmatrix} |L\rangle \\ |R\rangle \end{pmatrix}$ being the static field function; we construct the Hamiltonian of the system in matrix representation as

$$H = \psi^+\varepsilon(t)\,\psi + \psi^+ G\,\psi, \tag{16}$$

where, $\varepsilon(t) = \begin{pmatrix} \epsilon_0 + \alpha\beta(p - f(t)) & 0 \\ 0 & \epsilon_0 - \alpha\beta(p - f(t)) \end{pmatrix}$ and $G = \begin{pmatrix} 0 & \Delta_0(\alpha) \\ \Delta_0(\alpha) & 0 \end{pmatrix}$ are respectively the energy and tunneling matrix. The equation of motion is given as follows:

$$i\hbar\psi_{,0} = \varepsilon(t)\,\psi + G\,\psi.$$

Considering the transformation

$$\psi \to \exp\left(-\frac{i}{\hbar}\int_0^t \varepsilon(\tau)\,d\tau\right)\,\psi\,,$$

and with the help of the Campbell-Baker-Hausdorff Formula[74], the equation of motion expressed through the dynamic matrix is as follows

$$\psi_{,0} = \frac{1}{i\hbar}\exp\left(\frac{i}{\hbar}\int_0^t \varepsilon(\tau)\,d\tau\right) G \exp\left(-\frac{i}{\hbar}\int_0^t \varepsilon(\tau)\,d\tau\right)\psi,$$

where

$$\psi_{,0} = \frac{d\xi}{dt}\,\psi, \tag{17}$$

with the dynamic matrix being

$$\xi = \begin{pmatrix} 0 & a \\ -a^* & 0 \end{pmatrix}, \tag{18}$$

and

$$a = \int_{-\infty}^{t} \frac{\Delta_0(\alpha)}{i\hbar} \exp\left(\frac{2i\alpha\beta}{\hbar}\int (p - f(\tau))\, d\tau\right) d\tau,$$

We find the properties and exact solution of the transition matrix T^M of this problem. The analytical expression of T^M is obtained from the solution of:

$$\psi = T^M \psi_0 = \hat{T}\, \exp(\xi)\, \psi_0. \tag{19}$$

Where $\hat{T}$ is the time ordering operator. We remark that the Hamiltonian describes a periodic system. Therefore, if the transition matrix T^M describes the evolution of the system after a single period. The evolution after n periods is obtained as the n^{th} power of the transition matrix. Therefore, if T is the period and n an arbitrary integer,

$$\psi(T) = T^M \psi_0, \psi(nT) = \left(T^M\right)^n \psi_0,$$

$$\psi(nT + \tau) = \left(T^M\right)^n \psi(\tau),$$

Therefore, the main difficulty is to find out T^M for a single period. To analyse that term, we plot the diabatic and adiabatic energies of the system in Fig.4

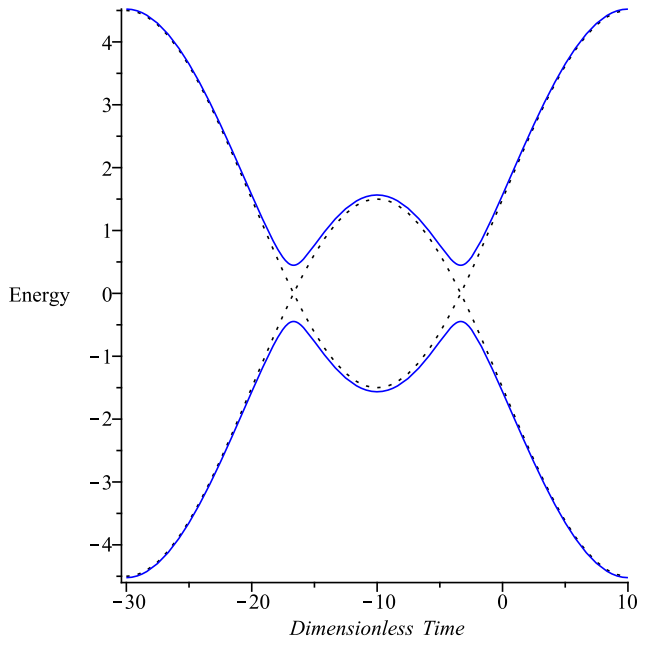

FIG. 4. Diabatic and adiabatic energies versus dimensionless time for a two-level configuration. The dotted black line are diabatic energy and the solid blue line are adiabatic energies.

It is seen that we have two crossings, the first playing the role of a beam splitter while the second recombine the energy lines giving rise to an interferometer. Such a system has been largely studied in the literature[53,57].

The time interval separating two crossings is known as relaxation time and conditions the appearence of interferences. For small relaxation time, the system undergoes a diabatic change resulting in a sudden death of the survival probability at the effective crossing point. The system mimics a single passage problem that resembles the so-called slow driving regime[51]. On the other hand, for large relaxation time, the system undergoes an adiabatic change and saturates prior to the second crossing thereby guaranteeing a survival probability. Here, the dynamic matrix of the system can be decomposed and reeordered in term of crossing time; the later mimics the so-called fast driving regime see ref.[51].

Therefore, the solution (19) can be reordered in terms of the two crossing times. The field vector of the system is given by

$$\psi = \hat{T} \exp(\xi_1(t)) \exp(\xi_2(t))\, \psi_0, \tag{20}$$

and the transition matrix

$$T^M = \hat{T} \exp(\xi_1(t)) \exp(\xi_2(t)), \tag{21}$$

with

$$\xi_1(t) = \begin{pmatrix} 0 & a \\ a^* & 0 \end{pmatrix}, \xi_2(t) = \begin{pmatrix} 0 & b \\ b^* & 0 \end{pmatrix},$$

$$a = \int_{-\infty}^{t} \frac{\Delta_0(\alpha)}{i\hbar} \exp\left(\frac{2i\alpha\beta}{\hbar}\int (p - f(\tau))\, d\tau\right) d\tau,$$

$$b = \int_{-\infty}^{t} \frac{\Delta_0(\alpha)}{i\hbar} \exp\left(\frac{2i\alpha\beta p\pi}{\hbar\Omega}\right) \exp\left(\frac{2i\alpha\beta}{\hbar}\int (p - f(\tau))\, d\tau\right) d\tau.$$

The action of the time ordering operator help in the derivation of the transition matrix of the system[50,75]; it is a 2×2 matrix with elements:

$$\left(T^M\right)_{11} = p_1 p_2 - q_1 q_2 \exp(-2i\,\Phi_{\rm ac}),$$

$$\left(T^M\right)_{12} = i\left(p_1 q_2 \exp(i\,\Phi_{\rm ac}) - q_1 p_2 \exp(-i\,\Phi_{\rm ac})\right) \exp(-i\,\Phi_0),$$

$$\left(T^M\right)_{21} = -\left(\left(T^M\right)_{12}\right)^*,\ \left(T^M\right)_{11} = \left(\left(T^M\right)_{22}\right)^*,$$

with

$$q_k = i\sqrt{1 - \exp\left(-2\pi\,\lambda_v\,\Lambda\left((-1)^k v, \frac{2\alpha\beta e_0}{\hbar\Omega}\right)\right)} \exp(i\phi_{\rm ks}),$$

$$p_k = \exp\left(-\pi\,\lambda_v\,\Lambda\left((-1)^k v, \frac{2\alpha\beta e_0}{\hbar\Omega}\right)\right),\ k = 1, 2,$$

$$v=\frac{2\alpha\beta p}{\hbar\Omega},\ \ 2\Phi_0=\phi_{2s}+\phi_{1s}+\pi v,$$

here, $2\Phi_{ac}=\phi_{2s}-\phi_{1s}+\pi v$ is the phase accumulated after the two passages, $\phi_{ks}=\lambda\ln\lambda+\lambda+\Gamma(i\lambda)$ is the Stock's phase of the k^{th} passage

$$\lambda_v=\frac{\Delta_0^2(\alpha)}{\hbar\Omega\,\alpha\beta e_0}\quad \lambda=\lambda_v\Lambda\left(v,\frac{2\alpha\beta e_0}{\hbar\Omega}\right). \tag{22}$$

are respectively the Landau-Zener and the renormalized Landau-Zener parameters of the system,

$$\Lambda\left(v,\frac{2\alpha\beta e_0}{\hbar\Omega}\right)=\frac{\pi\alpha\beta e_0}{\hbar\Omega}A_J^2\left(v,\frac{2\alpha\beta e_0}{\hbar\Omega}\right)+\frac{\pi\alpha\beta e_0}{\hbar\Omega}W_E^2\left(v,\frac{2\alpha\beta e_0}{\hbar\Omega}\right)$$

is the adiabatic power of the system that renormalizes the Landau-Zener parameter and appears as a consequence of the nonlinearity of energy level.

Under these considerations, the survival and transition probabilities of the system are respectively given by

$$P_s=\left(p_1p_2-q_1q_2\cos\left(2\Phi_{ac}\right)\right)^2+q_2^2q_1^2\sin^2\left(2\Phi_{ac}\right),$$

$$P_{tr}=q_1^2p_2^2+p_1^2q_2^2+2p_1p_2q_1q_2\cos\left(2\Phi_{ac}\right).$$

It is instructive to mention that the probability as well as the phase accumulated is different from one passage to another. In the particular case where the system is design in such a way that $p_1=p_2=p$ then the survival and transition probabilities become

$$P_s=\left(2p^2-1\right)^2+4p^2\left(1-p^2\right)\cos^2\left(\Phi_{st}\right),$$

$$P_{tr}=4p^2\left(1-p^2\right)\sin^2\left(\Phi_{st}\right),\ \Phi_{st}=\Phi_{ac}+\frac{\pi}{2}.$$

The system under this condition mimics a Landau-Zener-Stückelberg interferometer with the accumulated phase being the Stückelberg phase[51]. For the critical value $p=\frac{\sqrt{2}}{2}$, any anti-crossing behaves like a 50-50 beam splitter and the probabilities are given by

$$P_s=\cos^2\left(\Phi_{st}\right),\ \ P_{tr}=\sin^2\left(\Phi_{st}\right).$$

the system oscillates between the two basis states and the interference in this case is constructive. In the particular case where $v=2n$ (n being an integer), the two passages are identical and therefore for small values of the gap

$$\phi_{1s}-\phi_{2s}=0 \tag{23}$$

and the probabilities are given by

$$P_{tr}=4\exp\left(-2\pi\lambda_{2n}\Lambda\left(2n,\frac{2\alpha\beta e_0}{\hbar\Omega}\right)\right)\times\left(1-\exp\left(-2\pi\lambda_{2n}\Lambda\left(2n,\frac{2\alpha\beta e_0}{\hbar\Omega}\right)\right)\right)$$

$$P_s=\left(2\exp\left(-2\pi\lambda_{2n}\Lambda\left(2n,\frac{2\alpha\beta e_0}{\hbar\Omega}\right)\right)-1\right)^2.$$

The latter mimics the result derived by Zener in the double passage problem[76]. In a general frame, constructive interference will be observed when the imaginary part of the diagonal elements of the transition matrix tends to zero. Therefore the condition of appearance of constructive interference is resumed by

$$\phi_{2s}-\phi_{1s}+\pi v=\pi n,\ \ n=0,1,2,3,4... \tag{24}$$

Furthermore, the parameter v helps to control the style of interference. If v is an integer, the transitions are identical and the conditions above are almost satisfied. The plotting of survival and transition probabilities for constructive and destructive interferences are depicted on Figs. 5 and 6

Figs.5 and 6 show the plotting of survival and transition probabilities versus time for several periods and different values of parameters. From Fig.5, it is seen that after any crossing, the probability add up and enable the oscillation of probabilities between the two basis states (Stückelberg oscillations)[54,55]. The observation in Fig.5 show that, after any half-period even if two consecutive crossings can add up there will be a cancellation that destroys the construction of probabilities; the system can not oscillate between the two basis states and the interference is known as destructive. It can be seen that if v is an integer, the transitions under the same period are identical ($p_1=p_2$) and the phase accumulated become small. We register an oscillation of probabilities (see panel 5(a)); for some particular values of v, the second crossing behaves as a reflector but even in those cases the overall probability oscillates and the interference is still constructive. From another perspective, the types of interferences are conditioned by the parameter v; if v is an even integer, the interferences are purely constructive; the probabilities add up and we register an oscillation of probabilities. If v is an odd integer, the phase accumulated has a $(2n+1)\pi$ dephasing after a single passage. As a result, we register a certain sending back or cancelation after any construction, however, the overall probability oscillates around the two basis states with interferences being constructive. In the case where v is not an integer, the interferences are almost destructive unless condition (24) is satisfied. So the appearances of constructive and destructive interferences are controlled with the turnable parameters (p, L and C_j).

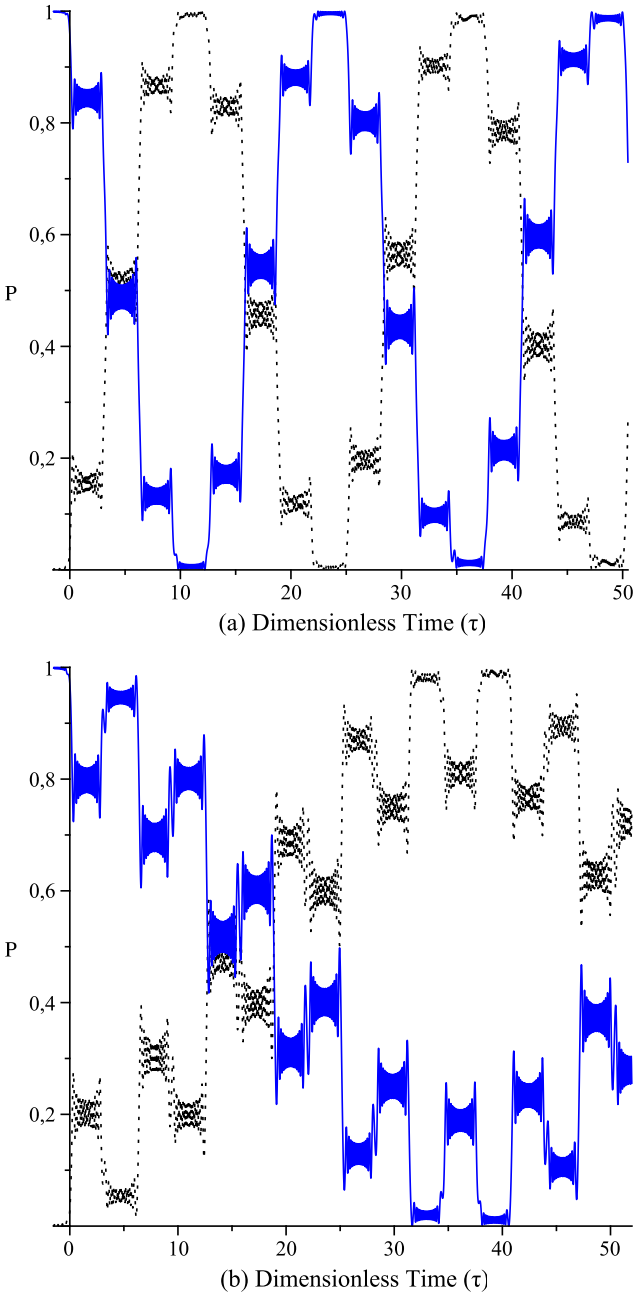

FIG. 5. Survival Probability (solid blue line) and transition probability (dotted-black line) versus dimensionless time (τ) for a two-level configuration (constructive interference) for parameters: (a) $v = 0$, $\frac{2\alpha\beta e_0}{\hbar\Omega} = \frac{180}{\pi}$;(b) $v = 3$, $\frac{2\alpha\beta e_0}{\hbar\Omega} = \frac{180}{\pi}$

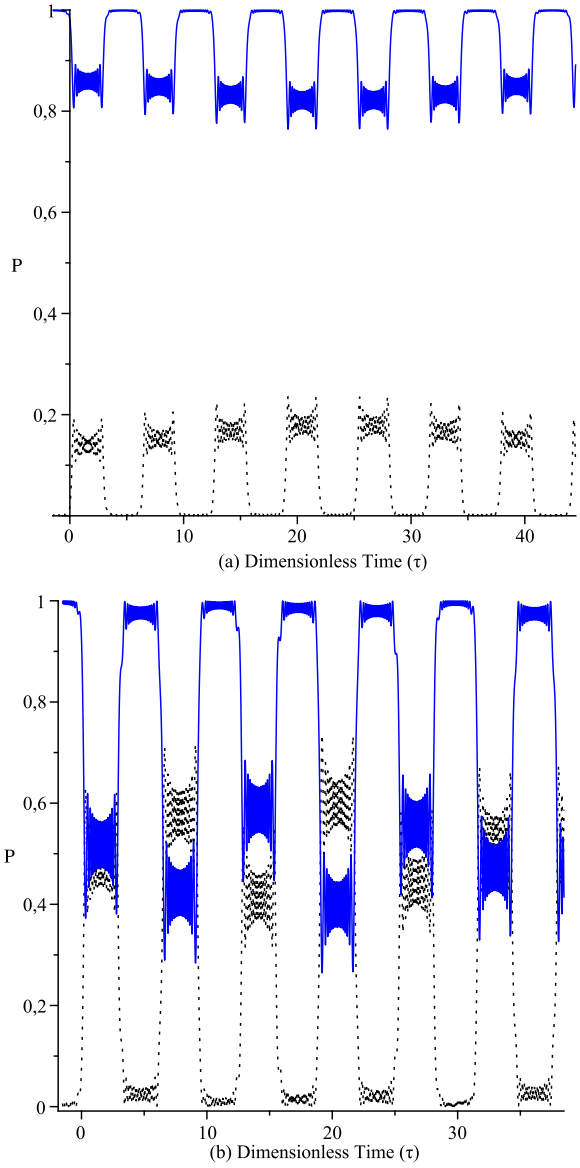

FIG. 6. Survival probability (solid blue line) and transition probability (dotted-black line) versus dimensionless time (τ) for a two-level configuration (destructive interference) for parameters: (a) $v = 1.25$, $\frac{2\alpha\beta e_0}{\hbar\Omega} = \frac{180}{\pi}$;(b) $v = 3.125$, $\frac{2\alpha\beta e_0}{\hbar\Omega} = \frac{180}{\pi}$

From another perspective, if the parameter v is larger than the oscillation amplitude ($p > e_0$) there is no crossing in the energy spectrum and therefore, no tunneling. A similar observation is achieved when we reduce the value of the inductance (L). Since the width of the barrier (2α) is an inverse proportion of the inductance, any enhancement in the inductance reduces the barrier width. The plotting of the probability limit for a single transition against the width of the barrier is depicted in Fig.7.

Fig.7 shows the variation of the probability limits for a single passage versus the width of the barrier; the observation of this figure shows that for small values of α the transition probability is unity while the survival probability is zero. This only highlights that by reducing the width of the barrier (enhancing L), we easily achieve a perfect transfer of the population. However, for large values of α the transition probability vanishes while the survival probability is unity. This materializes the complete blockage of the system achieved for large values of α. It is instructive to mention that, in this model, the total population transfer as well as the complete blockage are obtained in permissible range of parameters only by

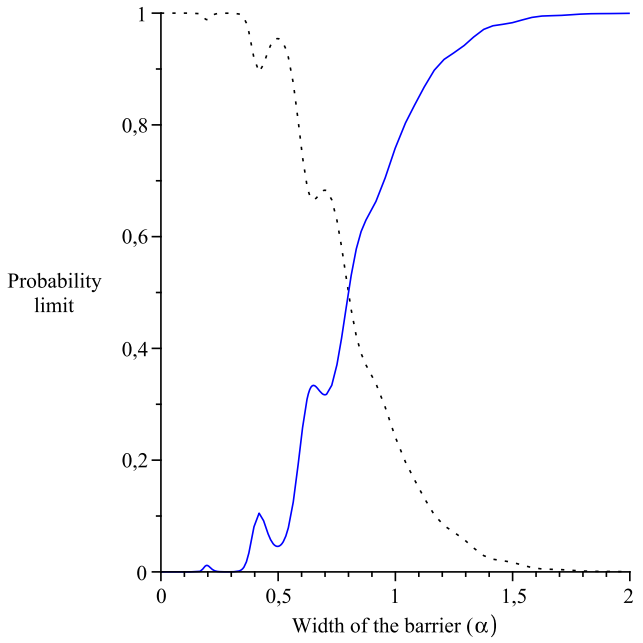

FIG. 7. Survival probability (solid blue line) and transition probability (dotted-black line) versus width of the barrier (α) in a two-level configuration

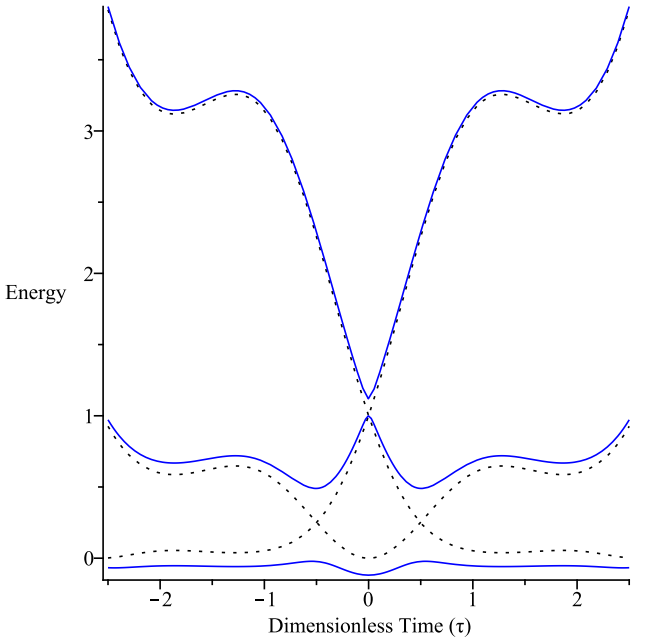

FIG. 8. Diabatic and adiabatic energies versus dimensionless time. The dotted black line are diabatic energy and the solid blue line are adiabatic energies.

changing the values of the inductance.

B. Three-level system

This configuration is obtained under the condition $\frac{2\mu}{\hbar^2}\beta a_1 \ll 1$ but with $a_1 \gg a_3$ where only the two relevant neighbouring states are considered. The Hamiltonian of the model is given by a 3×3 matrix:

$$\mathcal{H} = \begin{pmatrix} \epsilon_{-1} & \Delta_0 & 0 \\ \Delta_0 & \epsilon_0 & \Delta_0 \\ 0 & \Delta_0 & \epsilon_1 \end{pmatrix}.$$

with

$$\epsilon_m \sim \frac{\hbar m}{\mu}\left(\alpha\beta pt - \frac{\alpha\beta e_0}{\Omega}\cos(\Omega t)\right) + \frac{\hbar}{2\mu}\left(\alpha\beta pt - \frac{\alpha\beta e_0}{\Omega}\cos(\Omega t)\right)^2.$$

It can be seen that the energies of the system have both linear and a sinusoidal time dependence. The graphical representation of the diabatic and adiabatic energies is given in Fig.8.

This figure shows the plots of diabatic energies (dot black curves) as well as adiabatic (solid blue curves) as a function of the dimensionless time; The parameter that makes time dimensionless is: $\tau = \sqrt{\frac{\beta_0}{\hbar}}t$ ($\beta_0 = \frac{\hbar\alpha\beta p}{\mu}$). The system presents a single crossing and the probability of tunnelling through avoided crossing is the quantity of primary interests. This figure also shows the energy to be non-linear. The non-linearity may change the transition probability limit. When the system is driven slowly, it follows an adiabatic scenario; the resulting level crossing system is resumed by a three-level Landau-Zener problem. The investigation of the tunneling probability is done via dynamic matrix approach[52,75]. In order to find the transition probability, we use the Hamiltonian (13).

Considering $\psi_0 = \begin{pmatrix} |-1\rangle \\ |0\rangle \\ |1\rangle \end{pmatrix}$ being the static field function then,the energy and tunneling matrix are respectively given by

$$\varepsilon(t) = \begin{pmatrix} \epsilon_{-1} & 0 & 0 \\ 0 & \epsilon_0 & 0 \\ 0 & 0 & \epsilon_1 \end{pmatrix} \text{ and } G = \begin{pmatrix} 0 & \Delta_0 & 0 \\ \Delta_0 & 0 & \Delta_0 \\ 0 & \Delta_0 & 0 \end{pmatrix}$$

the master equation becomes

$$\psi_{,0} = \frac{d\xi}{dt}\psi, \tag{25}$$

with the dynamic matrix being

$$\xi = \begin{pmatrix} 0 & a & 0 \\ -a^* & 0 & b \\ 0 & -b^* & 0 \end{pmatrix}, \tag{26}$$

where

$$a = \int_{-\infty}^{t} \frac{\Delta}{i\hbar} \sum_{n=-\infty}^{n=+\infty} \mathrm{J}_n(z) \exp\left(\frac{i\beta_0\tau^2}{2\hbar} + v_{1n}\tau\right) d\tau,$$

$$b = \int_{-\infty}^{t} \frac{\Delta}{i\hbar} \sum_{n=-\infty}^{n=+\infty} \mathrm{J}_n(z) \exp\left(\frac{i\beta_0\tau^2}{2\hbar} + v_{2n}\tau\right) d\tau,$$

$$\beta_0 = \frac{\hbar\alpha\beta p}{\mu} \quad , \; v_{kn} = (-1)^k \frac{\hbar^2}{2\mu} + n\hbar\Omega, \quad z = \frac{\alpha\beta e_0}{\mu\,\Omega^2}.$$

The analytical expression of T^M is obtained from the solution of:

$$\psi = T^M\psi_0 = \hat{T}\,\exp(\xi)\,\psi_0, \tag{27}$$

where $\hat{T}$ is the time ordering operator. With the help of Wick's theorem and Dyson series[77–80], we compute the latter equation and obtain

$$\psi = \begin{bmatrix} {T^M}_{11} & {T^M}_{12} & {T^M}_{13} \\ {T^M}_{21} & {T^M}_{22} & {T^M}_{23} \\ {T^M}_{31} & {T^M}_{32} & {T^M}_{33} \end{bmatrix} \psi_0, \tag{28}$$

where

$${T^M}_{11} = 1 - \frac{\lambda_{00}}{\lambda_{00}+\lambda_1}\left(1 - \exp\left(-\pi\left(\lambda_{00}+\lambda_{01}\right)\right)\right),$$

$${T^M}_{12} = {T^{M^*}}_{21} = -\,i\left(\frac{\lambda_{00}}{\lambda_{00}+\lambda_{01}}\right)^{\frac{1}{2}} \times \sqrt{1-\exp\left(-2\pi\left(\lambda_{00}+\lambda_{01}\right)\right)},$$

$${T^M}_{13} = {T^{M^*}}_{31} = \frac{\sqrt{\lambda_{00}\lambda_{01}}}{\lambda_{00}+\lambda_{01}}\left(1-\exp\left(-\pi\left(\lambda_{00}+\lambda_{01}\right)\right)\right)$$

$${T^M}_{22} = \exp\left(-\pi\left(\lambda_{00}+\lambda_{01}\right)\right),$$

$${T^M}_{23} = {T^{M^*}}_{32} = -\,i\left(\frac{\lambda_1}{\lambda_{00}+\lambda_{01}}\right)^{\frac{1}{2}} \times \sqrt{1-\exp\left(-2\pi\left(\lambda_{00}+\lambda_{01}\right)\right)},$$

$${T^M}_{33} = 1 - \frac{\lambda_{01}}{\lambda_{00}+\lambda_{01}}\left(1-\exp\left(-\pi\left(\lambda_{00}+\lambda_{01}\right)\right)\right),$$

$$\pi\lambda_{00} = \left(aa^*\right)_{ord}, \;\; \pi\lambda_{01} = \left(bb^*\right)_{ord},$$

and the symbol *ord* representing the mean time order.

$$\lambda_{00} = \left|\sum_{-\infty}^{+\infty} \mathrm{J}_n(z) \exp\left(-\frac{iv_{1n}^2}{2\hbar\beta_0}\right)\right|^2, \tag{29}$$

$$\lambda_{11} = \left|\sum_{-\infty}^{+\infty} \mathrm{J}_n(z) \exp\left(-\frac{iv_{2n}^2}{2\hbar\beta_0}\right)\right|^2, \tag{30}$$

The field function of the system can now be written as

$$\psi = \begin{bmatrix} T_{11}^M & T_{12}^M & T_{13}^M \\ T_{21}^M & T_{22}^M & T_{32}^M \\ T_{31}^M & T_{32}^M & T_{33}^M \end{bmatrix} \begin{bmatrix} |-1\rangle \\ |0\rangle \\ |1\rangle \end{bmatrix}, \tag{31}$$

From the field vector (or transition matrix) above it is seen that the probable occupation varies with the initial occupied state; therefore, if the initial occupation is $|-1\rangle$, then the survival probability is given by the quantities

$$\begin{aligned} P_{s(-1\mapsto -1)} =& \left|T_{11}^M\right|^2 \\ =& \left(1 - \frac{\lambda_{00}}{\lambda_{00}+\lambda_{01}}\left(1-\exp\left(-\pi\left(\lambda_{00}+\lambda_{01}\right)\right)\right)\right)^2, \end{aligned}$$

while the transition probabilities of the system are

$$\begin{aligned} P_{-1\mapsto 0} =& \left|T_{12}^M\right|^2 \\ =& \frac{\lambda_{00}^2}{\left(\lambda_{00}+\lambda_{01}\right)^2}\left(1-\exp\left(-2\pi\left(\lambda_{00}+\lambda_{01}\right)\right)\right), \end{aligned}$$

$$\begin{aligned} P_{-1\mapsto 1} =& \left|T_{13}^M\right|^2 \\ =& \frac{\lambda_{00}\lambda_{01}}{\left(\lambda_{00}+\lambda_{01}\right)^2}\left(1-\exp\left(-\pi\left(\lambda_{00}+\lambda_{01}\right)\right)\right)^2, \end{aligned}$$

When the system is prepared in such a way that the initial occupation is $|0\rangle$, the survival probability is given by the quantities

$$\begin{aligned} P_{s(0\mapsto 0)} =& \left|T_{22}^M\right|^2 \\ =& \exp\left(-2\pi\left(\lambda_{00}+\lambda_{01}\right)\right), \end{aligned}$$

while the transition probabilities of the system are

$$P_{0\mapsto -1} = \left|T_{21}^M\right|^2 = \frac{\lambda_{00}}{\lambda_{00}+\lambda_{01}}\left(1-\exp\left(-2\pi\left(\lambda_{00}+\lambda_{01}\right)\right)\right),$$

$$P_{0\mapsto 1} = \left|T_{23}^M\right|^2 = \frac{\lambda_1}{\lambda_{00}+\lambda_{01}}\left(1-\exp\left(-2\pi\left(\lambda_{00}+\lambda_{01}\right)\right)\right),$$

The last case is the most relevant since for any central lobe, we have two relevant lobes. The multi-crossing behaviour is obtained when the relaxation time v, which depends on the external capacitor, is large. In fact, the system carries intrinsically a multiple crossing behaviour. If the relaxation time v is small, the induced energy gap $J_n(z)$ operates in a really small time interval; therefore fictitious crossings are not expected. However, if v is large, the induced energy gaps around $n = 0$ mean

that $...J_{-2}(z), J_{-1}(z), J_1(z), J_2(z)...$ operate separately. Therefore, the system behaves at each of these points as if they where an anti-crossing (avoided crossing); the fictitious crossing are expected and the probability changes drastically[52,75].

The survival probability as function of dimensionless time for different values of v is illustrated in Fig.9.

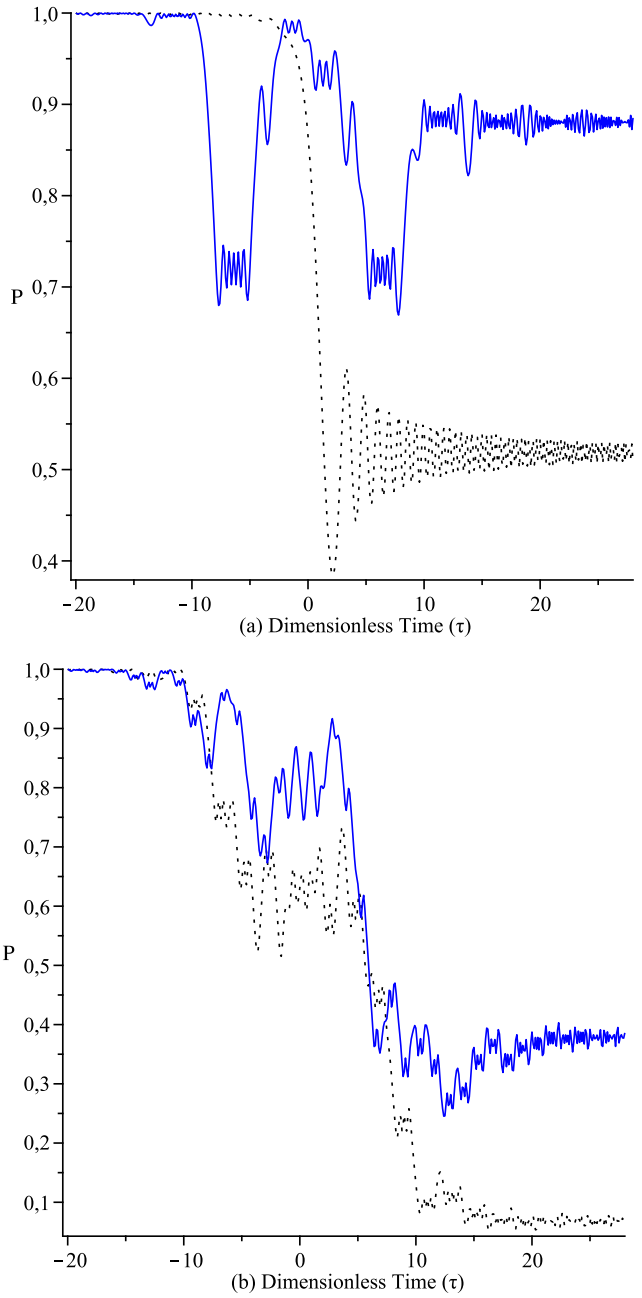

FIG. 9. Survival probability (solid blue line) and transition probability (dotted-black line) versus dimensionless time (τ) for a two-level configuration (constructive interference) for parameters: (a) $v = 0, v = 1.25$ $\frac{2\alpha\beta e_0}{\hbar\Omega} = \frac{180}{\pi}$;(b) $v = 3, v = 5$, $\frac{2\alpha\beta e_0}{\hbar\Omega} = \frac{180}{\pi}$

Fig.9 shows the variation of the survival probability as a function of time for different values of v. It is observed that as v increases, we register a drastic change in the values of the probabilities. This phenomenon can easily be understood when the notion of fictitious crossings is introduced. In fact, for small relaxation time, the system does not have time to adapt to change before it faces the next crossing. Therefore each of the induced gap adds in complimentary manner and it results in a deep fall in survival probability at the effective crossing point (see Fig.9.a, dotted black curve).

In the case of large relaxation time, the system after facing the first crossing adapts to the change imposed, and saturates before it comes to the next crossing; each of the induced gaps adds separately and because of the phase accumulated after each of these crossing, the transition probabilities can be constructed or destroyed and the overall is the probability limit. From the energy time diagram, the system presents only three crossings. for small relaxation those three crossings occur at around $t = 0$; this is justified by the single crossing observed on the diagram Fig.9.a, (dotted black curve). For large relaxation, additionally to the two crossings observed on energy curves, we have many other ones. Since they are not part of the energy diagram, they are known as fictitious crossings. Their appearance is conditioned by the relaxation time v and the effective gap $\Delta J_n(z)$. Observing the solid blue line of Fig.9, we can count the number of crossings in the system; this is due to the fact that the gap $\Delta J_n(z)$ decays as n increases. Therefore, when n is large, the gap vanishes and the probability saturates.

C. Multi-level system

Here, we consider the same situation as previously (section 3.B) but, we take into consideration all relevant states. So $\beta a_1 \frac{2\mu}{\hbar^2} << 1$ and the Hamiltonian of the system is labeled as in Eq.12

$$H = \sum_m \epsilon_m |m\rangle\langle m| + \Delta|m+1\rangle\langle m| + \Delta|m-1\rangle\langle m|.$$

The field vector of the system is given by:

$$\psi = \begin{pmatrix} C_{-l} \\ C_{-l+1} \\ \vdots \\ C_l \end{pmatrix},$$

with $l \longrightarrow +\infty$; we then have an infinite number of relevant states. The evaluation of the dynamic matrix in this case is via:

$$i\hbar\psi_{,0} = H\psi_0. \tag{32}$$

The transition amplitude C_m can be generalized as a single differential equation

$$i\hbar\dot{C}_m = \epsilon_m C_m + \Delta\left(C_{m+1} + C_{m-1}\right). \tag{33}$$

with $m = -l \ldots\ldots l$, $l \longrightarrow +\infty$. Because of the infinite number of values taken by m, we can rewrite that equation in terms of

$$i\hbar\psi_{,0} = \epsilon_m\psi + \Delta\left(J_+ + J_-\right)\psi. \tag{34}$$

where

$$\epsilon_m \sim \frac{m}{2}\epsilon\left(t\right) + \frac{1}{2}\epsilon_0\left(t\right),$$

is the elements of the energy matrix ε and so $\varepsilon_{m,n} = \epsilon_m\delta_{m,n}$ and

$$\epsilon\left(t\right) = (\beta_0 t - z\Omega\cos\left(\Omega t\right)),$$

$$\epsilon_0\left(t\right) = (\beta_0 t - z\Omega\cos\left(\Omega t\right))^2,$$

The term $\Delta\left(J_+ + J_-\right)$ represents the tunneling matrix. Here,

$$J_+ = \begin{pmatrix} 0 & 1 & 0 & 0 & 0 & 0 & \ldots \\ 0 & 0 & 1 & 0 & 0 & 0 & \ldots \\ 0 & 0 & 0 & 1 & 0 & 0 & \ldots \\ 0 & 0 & 0 & 0 & 1 & 0 & \ldots \\ 0 & 0 & 0 & 0 & 0 & 1 & \ldots \\ 0 & 0 & 0 & 0 & 0 & 0 & \ldots \\ \vdots & \vdots & \vdots & \vdots & \vdots & \vdots & \ddots \end{pmatrix},$$

is an upper triangular matrix while

$J_- = (J_+)^t$ is a lower triangular matrix with constant elements 1. Moreover, J_+ and J_- are shifting operators acting on the k space. Taking that

$$\psi = \exp\left(i\int\varepsilon\left(t\right)dt\right)M$$

Then eq.(34) is reduced as

$$\dot{M} = \frac{d}{dt}\left(\alpha\left(t\right)J_+ - \beta\left(t\right)J_-\right)M. \tag{35}$$

with

$$\Xi\left(t\right) = \int_{-\infty}^{t}\frac{\Delta}{i\hbar}\exp\left(\frac{i}{\hbar}\int_{-\infty}^{t'}\epsilon_m\left(\tau\right) - \epsilon_{m-1}\left(\tau'\right)d\tau\right)dt'.$$

and

$$\Upsilon\left(t\right) = \int_{-\infty}^{t}\frac{\Delta}{i\hbar}\exp\left(\frac{i}{\hbar}\int_{-\infty}^{t'}\epsilon_m\left(\tau\right) - \epsilon_{m+1}\left(\tau'\right)d\tau\right)dt'.$$

So the dynamics matrix is expressed by

$$\xi = \Xi\left(t\right)J_+ - \Upsilon\left(t\right)J_-. \tag{36}$$

and the solution is obtained as:

$$M = \widehat{T}\exp\left(\xi\right)M_{-\infty}. \tag{37}$$

or

$$M = \widehat{T}\exp\left(\Xi\left(t\right)J_+ - \Upsilon\left(t\right)J_-\right)M_{-\infty}. \tag{38}$$

from the above solution , the transition matrix is given by:

$$T^M = \widehat{T}\exp\left(\Xi\left(t\right)J_+ - \Upsilon\left(t\right)J_-\right)M_{-\infty}. \tag{39}$$

The solution is therefore being rewritten in terms of the state vector ψ

$$\psi = \exp\left(\frac{i}{\hbar}\int\varepsilon\left(t\right)dt\right).\widehat{T}\exp\left(\alpha\left(t\right)J_+ - \beta\left(t\right)J_-\right)M_{-\infty}. \tag{40}$$

Taking into consideration that the operators J_+ and J_- and $\widehat{m}$ obey to the following commutation relation:

$$[J_\pm, \widehat{m}] = \pm J_\pm.$$

we use Dyson ordering or Magnus expansion to evaluate the transition matrix[50,73,81];

taking $M_{-\infty} = \sum_k C_m\delta_{km}$, then the elements of the field vector are:

$$C_m = \sum_k C_k\exp\left(\frac{ik}{\hbar}\int_{-\infty}^{t}\epsilon_0\left(\tau\right) + \epsilon_0\left(\tau\right)d\tau\right) \times\left(\frac{\Xi(t)}{\Upsilon(t)}\right)^{\frac{m-k}{2}}J_{m-k}[2\sqrt{\alpha(t)\beta(t)}].$$

Taking that $C_m(-\infty) = \delta_{m0}$ then

$$C_m = \exp\left(\frac{i}{\hbar}\int_{-\infty}^{t}\epsilon\left(\tau\right) + \epsilon_0\left(\tau\right)d\tau\right)\left(\frac{\Xi(t)}{\Upsilon(t)}\right)^{\frac{l}{2}} \times J_l[2\sqrt{\alpha(t)\beta(t)}].$$

this gives us the generalized transition amplitude for an arbitrary state $|m\rangle$ where the probabilities are found as the square of modulus.

V. CONCLUSION

In this paper, we have studied a modified Josephson junction based circuit and the resulting Landau-Zener scenario. We show that the Josephson junction based circuit can be modeled as a multi-level system with crossing energy levels. Two particular cases emerge from our studies. If the charging energy of the junction is larger than the energy stored in the junction, the system mimics

a multi-level system. The special case of nearest neighbor approximation leads to a three-level system where the Landau-Zener transition probabilities are determined. In the case where all relevant states are considered, the probability amplitude are given in terms of the Bessel function of first kind.

It is seen that, the capacitance of the capacitor parallel to the Josephson junction component C_j is the controllable parameter that conditions the value of the charging energy $\frac{\hbar^2}{2\mu}$ as well as the energy stored in the junction βa_1 through parameters β and μ. The inductance of the coil L parallel to the Josephson junction component is the controllable parameter that conditions the shape of the potential energy and therefore the level configuration through the a_3 parameter. The parameter p carries the initial condition in the inductive branch. This is helpful for the design of constructive and destructive interferences through the parameter υ

We prove that, when the charging energy of the junction is less than the energy stored in the junction, the system mimics a two-level system where the confining potential is lifted as a double well potential. This is achieved by enhancing the capacitance C_{0j} as well as the inductance L . Observing the evolution of the system as a function of time we can see the influence of the initial conditions on the type of interference. Thus if (υ) is an even number, the interference is purely constructive and the probability oscillates with high frequency. When (υ) is odd, it appears a certain phase opposition between two successive crossings. However,the overall probability oscillates at very low frequency and the interference are still constructive. When (υ) is not an integer, the transitions are not identical; the transition probabilities of two successive transitions are different and the interferences are destructive. Therefore, playing on the initial condition p and the inductance L, we can set the type of interference while the value of the inductance controls the value of the gap as well as the frequency of the probability. Moreover, the nonlinearity of energy levels modifies the transition probability and the derived adiabatic parameters help to redefine the Landau-Zener probability. Therefore, the total population transfer as well as the complete blocking of the system are obtained in a permissible range of parameters only by changing the values of the inductance.

Moreover, the total population transfer as well as the complete blockage of the system are obtained in the permissible range of parameters only by changing the values of the inductance. Therefore, the system models a controllable level-crossing system where the additional branches (inductive and capacitive) helps to design the number of levels, the type of interferometry as well as the control of level's occupation.

VI. DATA AVAILABILITY STATEMENT

The data that supports the findings of this study are available within this article.

VII. ACKNOWLEDGEMENTS

HAC thanks ICTP-SAIFR and FAPESP grant 2011/11973-4 for partial support. P.L. acknowledges support by the FAPESP Grant No. 2014/13272-1.

[1] B. Josephson, Physics Letters **1**, 251 (1962).
[2] H. Asai, Y. Ota, S. Kawabata, M. Machida, and F. Nori, Physical Review B **89** (2014), 10.1103/physrevb.89.224507.
[3] A. Barone and G. Paternò, *Physics and Applications of the Josephson Effect* (Wiley, 1982).
[4] P. W. Anderson and J. M. Rowell, Physical Review Letters **10**, 230 (1963).
[5] S. Shapiro, Physical Review Letters **11**, 80 (1963).
[6] B. Jäck, M. Eltschka, M. Assig, A. Hardock, M. Etzkorn, C. R. Ast, and K. Kern, Applied Physics Letters **106**, 013109 (2015).
[7] A. M. van den Brink, A. A. Odintsov, P. A. Bobbert, and G. Schön, Zeitschrift für Physik B Condensed Matter **85**, 459 (1991).
[8] O. Vávra, R. Soni, A. Petraru, N. Himmel, I. Vávra, J. Fabian, H. Kohlstedt, and C. Strunk, AIP Advances **7**, 025008 (2017).
[9] G. Paternò, A. M. Cucolo, and G. Modestino, Journal of Applied Physics **57**, 1680 (1985).
[10] R. W. Gurney and E. U. Condon, Physical Review **33**, 127 (1929).
[11] J. Taylor, *Modern physics for scientists and engineers* (Pearson Prentice Hall, Upper Saddle River, NJ, 2004).
[12] J. B. Rommel, Y. Liu, H.-J. Werner, and J. Kästner, The Journal of Physical Chemistry B **116**, 13682 (2012).
[13] A. J. Leggett, Physical Review B **30**, 1208 (1984).
[14] E. Simánek, Oxford University Press **32**, 1137 (1994).
[15] S. Takagi, *Macroscopic quantum tunneling* (Cambridge University Press, 2002).
[16] U. Weiss, *Quantum dissipative systems* (World scientific, 2012).
[17] F. Tafuri, *Fundamentals and Frontiers of the Josephson Effect* (Springer-Verlag GmbH, 2019).
[18] T. Kato and M. Imada, Journal of the Physical Society of Japan **65**, 2963 (1996).
[19] S. Kawabata, S. Kashiwaya, Y. Asano, and Y. Tanaka, Physical Review B **72** (2005), 10.1103/physrevb.72.052506.
[20] M. Machida and T. Koyama, Physica C: Superconductivity and its Applications **463-465**, 84 (2007).
[21] S. Savel'ev, A. L. Rakhmanov, and F. Nori, Physical Review Letters **98** (2007), 10.1103/physrevlett.98.077002.
[22] A. O. Sboychakov, S. Savelev, A. L. Rakhmanov, and F. Nori, Europhysics Letters (EPL) **80**, 17009 (2007).
[23] A. O. Sboychakov, S. Savel'ev, and F. Nori, Physical Review B **78** (2008), 10.1103/physrevb.78.134518.
[24] S. Savel'ev, A. O. Sboychakov, A. L. Rakhmanov, and F. Nori, Physical Review B **77** (2008), 10.1103/physrevb.77.014509.
[25] S. Kawabata, T. Bauch, and T. Kato, Physical Review B **80** (2009), 10.1103/physrevb.80.174513.
[26] Y. Ota, M. Machida, and T. Koyama, Physical Review B **83** (2011), 10.1103/physrevb.83.060503.
[27] R. Leoni, P. Carelli, and V. Foglietti, Journal of Applied Physics **64**, 2527 (1988).
[28] M. F. G. Zalba, J. Haigh, T.-Y. Yang, and L. Ibberson, Hitachi Review **68**, 548 (2019).
[29] R. Vrijen, E. Yablonovitch, K. Wang, H. W. Jiang, A. Balandin, V. Roychowdhury, T. Mor, and D. DiVincenzo, Physical Review A **62** (2000), 10.1103/physreva.62.012306.
[30] M. H. Devoret and R. J. Schoelkopf, Science **339**, 1169 (2013).
[31] G. Wendin and V. Shumeiko, in *Fundamentals and Frontiers of the Josephson Effect*, Vol. 33 (Low Temperature Physics, American Institute of Physics, 2007) pp. 724–744.
[32] Y. Makhlin, G. Schön, and A. Shnirman, Reviews of Modern Physics **73**, 357 (2001).
[33] J. Mooij, T. Orlando, L. Levitov, L. Tian, C. H. Van der Wal, and S. Lloyd, Science **285**, 1036 (1999).

[34]Y. Nakamura, Y. A. Pashkin, and J. S. Tsai, Nature **398**, 786 (1999).
[35]M. Sillanpää, T. Lehtinen, A. Paila, Y. Makhlin, and P. Hakonen, Physical Review Letters **96** (2006), 10.1103/physrevlett.96.187002.
[36]K. Bladh, T. Duty, D. Gunnarsson, and P. Delsing, New Journal of Physics **7**, 180 (2005).
[37]M. Steffen, J. M. Martinis, and I. L. Chuang, Physical Review B **68** (2003), 10.1103/physrevb.68.224518.
[38]L. D. Landau, Zeitschrift fur Physik (Sowjetunion) **2**, 118 (1932).
[39]C. Zener, Proceedings of the Royal Society of London. Series A, Containing Papers of a Mathematical and Physical Character **137**, 696 (1932).
[40]A. Sibille, J. F. Palmier, and F. Laruelle, Physical Review Letters **80**, 4506 (1998).
[41]K. Mullen, E. Ben-Jacob, and Z. Schuss, Physical Review Letters **60**, 1097 (1988).
[42]B. Wu and Q. Niu, Physical Review A **61** (2000), 10.1103/physreva.61.023402.
[43]J. Liu, L. Fu, B.-Y. Ou, S.-G. Chen, D.-I. Choi, B. Wu, and Q. Niu, Physical Review A **66** (2002), 10.1103/physreva.66.023404.
[44]Y.-A. Chen, S. D. Huber, S. Trotzky, I. Bloch, and E. Altman, Nature Physics **7**, 61 (2010).
[45]D. Suqing, L.-B. Fu, J. Liu, and X.-G. Zhao, Physics Letters A **346**, 315 (2005).
[46]G.-F. Wang, L.-B. Fu, and J. Liu, Physical Review A **73** (2006), 10.1103/physreva.73.013619.
[47]S. Raghavan, A. Smerzi, S. Fantoni, and S. R. Shenoy, Physical Review A **59**, 620 (1999).
[48]O. Zobay and B. M. Garraway, Physical Review A **61** (2000), 10.1103/physreva.61.033603.
[49]G.-F. Wang, D.-F. Ye, L.-B. Fu, X.-Z. Chen, and J. Liu, Physical Review A **74** (2006), 10.1103/physreva.74.033414.
[50]M. Jipdi, M. Tchoffo, and L. Fai, Physica E: Low-dimensional Systems and Nanostructures **96**, 36 (2018).
[51]S. Shevchenko, S. Ashhab, and F. Nori, Physics Reports **492**, 1 (2010).
[52]M. Jipdi, L. Fai, and M. Tchoffo, Physics Letters A **380**, 3665 (2016).
[53]J.-N. Zhang, C.-P. Sun, S. Yi, and F. Nori, Physical Review A **83** (2011), 10.1103/physreva.83.033614.
[54]E. Stückelberg, Helv. Phys. Acta,(Basel) **5**, 369 (1932).
[55]E. Majorana, Il Nuovo Cimento **9**, 43 (1932).
[56]L.-K. Lim, J.-N. Fuchs, and G. Montambaux, Physical Review A **91** (2015), 10.1103/physreva.91.042119.
[57]X. Tan, D.-W. Zhang, Z. Zhang, Y. Yu, S. Han, and S.-L. Zhu, Physical Review Letters **112** (2014), 10.1103/physrevlett.112.027001.
[58]G. D. Fuchs, V. V. Dobrovitski, D. M. Toyli, F. J. Heremans, and D. D. Awschalom, Science **326**, 1520 (2009).
[59]H. Ribeiro and G. Burkard, Physical Review Letters **102** (2009), 10.1103/physrevlett.102.216802.
[60]J. R. Petta, H. Lu, and A. Gossard, Science **327**, 669 (2010).
[61]L. Wang, T. Tu, B. Gong, C. Zhou, and G.-C. Guo, Scientific Reports **6** (2016), 10.1038/srep19048.
[62]P. Louodop, R. Tchitnga, F. F. Fagundes, M. Kountchou, V. K. Tamba, C. L. P. L., and H. A. Cerdeira, Physical Review E **99** (2019), 10.1103/physreve.99.042208.
[63]H. Sun, S. K. Scott, and K. Showalter, Physical Review E **60**, 3876 (1999).
[64]T. Hongray, J. Balakrishnan, and S. K. Dana, Chaos: An Interdisciplinary Journal of Nonlinear Science (2015).
[65]A. Mishra, S. Saha, C. Hens, P. K. Roy, M. Bose, P. Louodop, H. A. Cerdeira, and S. K. Dana, Physical Review E **95** (2017), 10.1103/physreve.95.010201.
[66]D. Domínguez and H. A. Cerdeira, Physical Review B **52**, 513 (1995).
[67]D. Domínguez and H. A. Cerdeira, Physical Review Letters **71**, 3359 (1993).
[68]D. Domínguez and H. A. Cerdeira, Physics Letters A **200**, 43 (1995).
[69]A. O. Caldeira, *An Introduction to Macroscopic Quantum Phenomena and Quantum Dissipation* (Cambridge University Press, 2009).
[70]H. Hochstadt, *Special Functions of Mathematical Physics Hardcover* (Holt, Rinehart and Winston, 1961).
[71]M. Ayub, K. Naseer, M. Ali, and F. Saif, Journal of Russian Laser Research **30**, 205 (2009).
[72]M. Doncheski and R. Robinett, Annals of Physics **308**, 578 (2003).
[73]G. Dattoli, J. C. Gallardo, and A. Torre, La Rivista Del Nuovo Cimento Series 3 **11**, 1 (1988).
[74]J.-L. Loday, A. Frabetti, F. Chapoton, and F. Goichot, *Dialgebras and related operads, volume 1763 of Lecture Notes in Mathematics* (Springer-Verlag, Berlin, 2001).
[75]L. C. Fai, M. Tchoffo, and M. N. Jipdi, The European Physical Journal Plus **130** (2015), 10.1140/epjp/i2015-15071-y.
[76]M. Ateuafack, J. Diffo, and L. Fai, Physica B: Condensed Matter **483**, 37 (2016).
[77]I. DOKAS, Glasgow Mathematical Journal **52**, 303 (2009).
[78]J.-C. Novelli and J.-Y. Thibon, Advances in Applied Mathematics **40**, 8 (2008).
[79]G. C. Wick, Physical Review **80**, 268 (1950).
[80]M. Bauer, R. Chetrite, K. Ebrahimi-Fard, and F. Patras, Letters in Mathematical Physics **103**, 331 (2012).
[81]G. Dattoli and A. Torre, Journal of Mathematical Physics **28**, 618 (1987).